Eur. Phys. J. B **22**, 79–87 (2001)

THE EUROPEAN PHYSICAL JOURNAL B

EDP Sciences

Two-dimensional dilute Bose gas in the normal phase

P. Pieri[a], G.C. Strinati, and I. Tifrea[b]

Dipartimento di Matematica e Fisica, Sezione INFM, Università di Camerino, 62032 Camerino, Italy

Received 3 March 2001 and Received in final form 9 April 2001

Abstract. We consider a two-dimensional dilute Bose gas above its superfluid transition temperature. We show that the t-matrix approximation corresponds to the leading set of diagrams in the dilute limit, provided the temperature is sufficiently larger than the superfluid transition temperature. Within this approximation, we give an explicit expression for the wave-vector and frequency dependence of the self-energy, and calculate the corrections to the chemical potential and the effective mass arising from the interaction. We also argue that the breakdown of diagrammatic classification scheme for the dilute Bose gas, which occurs upon lowering the temperature, provides a criterion to estimate an upper bound for the superfluid critical temperature. The upper bound to the critical temperature identified by this criterion turns out to coincide with earlier results for the critical temperature obtained by Popov and by Fisher and Hohenberg using different methods. Extension of this procedure to the three-dimensional case gives good agreement with recent Monte Carlo data.

PACS. 05.30.Jp Boson systems – 05.70.Fh Phase transitions: general studies – 03.75.Fi Phase coherent atomic ensembles; quantum condensation phenomena

1 Introduction

Renewed interest in two-dimensional (2D) superfluid systems has been recently prompted by the discovery of high-temperature superconductors. Before that, studying 2D bosonic systems was mainly motivated by experiments on adsorbed helium monolayers [1] and spin-polarized hydrogen recombining on a helium film [2]. More recently, Bose condensation has been achieved experimentally in dilute gases of alkali atoms [3] and in atomic hydrogen [4], stimulating active research in this field both experimentally and theoretically [5].

Even though Bose-Einstein condensation is known not to occur at finite temperature for the ideal and interacting boson systems both in one and two dimensions, the absence of a condensate does not necessarily imply the lack of a phase transition to a superfluid state for an interacting 2D Bose system [6]. In this system, particles with small momenta behave like a condensate and are responsible for the presence of a nonvanishing superfluid density [7]. The critical temperature for the superfluid phase transition was estimated by Popov [7] using a functional integral formalism. The same estimate for the critical temperature was later obtained by Fisher and Hohenberg [8] using a renormalization-group approach, with the result

$$T_{\rm c} \approx \frac{2\pi n}{m \ln \ln \left[1/(n r_0^2)\right]} \,, \tag{1}$$

where n is the particle density, m the boson mass, and r_0 the range of the interaction potential between bosons (we set $\hbar = k_{\rm B} = 1$ throughout). In these studies, Popov [7] and Fisher and Hohenberg [8] approached the phase transition from the superfluid phase and the normal phase, respectively.

The present paper studies the 2D *dilute* Bose gas *above its critical temperature* $T_{\rm c}$ by relying on conventional diagrammatic methods. (The criterion for a 2D Bose system to be "dilute" will be specified below.) In this way, results for thermodynamic quantities are most readily obtained. In addition, these results are amenable to extension to more complex systems, such as the composite bosons occurring in the BCS to Bose-Einstein crossover problem [9]. Finally, our method enables us to treat on equal footing the dilute Bose gas both in two *and* three dimensions.

Previous studies of the 2D dilute Bose gas have considered the superfluid phase either at zero temperature [10–13] or at finite temperature [7,14]. At finite temperature, the absence of a condensate in 2D required either the separation of wave-vector integration into rapid and slow parts [7], or the use of appropriate renormalization group methods [14]. Previous approaches to the 2D dilute Bose gas, however, did not address the following issues: (i) The complete description of the normal phase (above the critical temperature) by standard diagrammatic

[a] e-mail: pieri@campus.unicam.it

[b] *Permanent address*: Dept. of Theoretical Physics, "Babes-Bolyai" University, 3400 Cluj, Romania

methods (to obtain the wave-vector and frequency dependence of the self-energy, the effective mass, and the chemical potential); (ii) Upon lowering the temperature, the detection by these methods of the insurgence of a superfluid phase transition *not* associated with the establishing of long-range order.

In this respect, standard many-body diagrammatic methods prove sufficient for a complete description of the normal phase of the 2D dilute Bose gas. In particular, the t-matrix approximation for the self-energy will be shown to provide the correct description for a dilute Bose gas above T_c, akin to the three-dimensional (3D) case. Both in 2D and in 3D, an explicit analytic expression for the self-energy as a function of wave vector and frequency will be presented.

In our approach, an expression like (1) appears as a *lower bound* for the validity of the t-matrix as a *controlled* approximation for the dilute Bose gas. The ensuing diagrammatic classification scheme for the dilute Bose gas will, in fact, be shown to break down when the temperature T approaches *a lower temperature* T_L, whose expression turns out to coincide with the estimate (1) for the critical temperature given in references [7] and [8]. We argue that the insurgence of the (superfluid) phase transition enters the diagrammatic theory for the dilute Bose gas in this way, since the physical mechanism leading to a breakdown of diagrammatic perturbation theory can only be the occurrence of a phase transition. Indeed, the classification scheme for the dilute Bose gas is based on the effective range of the interaction being smaller than the interparticle distance. Its breakdown, therefore, has to be ascribed to the insurgence of a new length scale which becomes increasingly large upon lowering the temperature. Such an increasing length scale upon lowering the temperature finds a natural explanation as a correlation length associated to a (second-order) phase transition. The temperature T_L is thus expected to provide *an upper boundary* of the critical region about the critical temperature T_c. (From a technical point of view, the coincidence of our result for T_L with the previous result (1) for T_c is due to the fact that both our approach and the previous ones discard sublogarithmic corrections to T_L and T_c, respectively.) It should be also emphasized that our method, which holds irrespective of the kind of order parameter that might be identified below T_c, is able to detect the occurrence of a phase transition but not to identify its nature. On the other hand, the very fact that our method does not depend on the kind of an order parameter below T_c (or even its existence), implies that this method is very general and that it can be adopted with no modifications both in 2D and 3D, whereby an order parameter cannot (D = 2) or can (D = 3) be identified. For the 3D case we obtain $(T_L - T_{BE})/T_{BE} \sim n^{1/3}a$ (where T_{BE} is the 3D Bose-Einstein temperature and a is the scattering length), in agreement with recent Monte Carlo simulations [15,16] for the 3D dilute Bose gas which yield for the critical temperature T_c a value which is slightly smaller than what we obtain for T_L.

The paper is organised as follows. Section 2 sets up the diagrammatic theory for the 2D dilute Bose gas in the normal phase and calculates the corrections to the chemical potential and the effective mass due to the interaction. Section 3 discusses the insurgence of a phase transition for the dilute Bose gas through the breakdown of the approximation scheme introduced in Section 2. The value of the breakdown-temperature T_L is then calculated both in two and three dimensions. Section 4 gives our conclusions. In the Appendix, the full dependence of the t-matrix self-energy on wave vector and frequency is obtained both in 2D and in 3D, by exploiting the diluteness condition. In addition, the validity of some approximations, on which the theoretical arguments of the text rely, is explicitly tested numerically.

2 T-matrix approximation for a dilute system of interacting bosons

In this section, we analyze the diagrammatic theory for the 2D Bose gas in the normal phase and determine the leading contributions to the self-energy in the dilute limit. We give an analytic expression for the wave-vector and frequency dependence of the self-energy, which becomes asymptotically exact in the dilute limit (as verified in the Appendix). We further use the zero wave-vector and frequency value of this self-energy to dress the single-particle Green's functions of the theory in a self-consistent way. This step will enable us to identify a *lower* temperature T_L below which the classification of diagrams for the dilute Bose system breaks down, as discussed in the next section. In addition, we obtain the explicit leading corrections to the chemical potential μ due to interaction, thus recovering an earlier result by Popov [7], and to the effective mass.

We begin by considering a 2D bosonic system interacting *via* a *short-range* two-body potential $v(\mathbf{r})$ with a finite range r_0, which becomes a δ-function when $r_0 \to 0$ (*cf.* Ref. [12]). (For the explicit solution of the t-matrix integral equation, in the Appendix we shall use a separable potential in wave-vector space in the place of the original short-range potential $v(\mathbf{r})$. This replacement will be fully justified.) We examine the *dilute* limit of this system, which is initially identified by the condition $nr_0^2 \ll 1$, where n is the bosonic density. (A stronger condition on the parameter nr_0^2 will be required below.) We further consider temperatures *above* a nominal critical temperature T_c but lower than an upper temperature of the order of $T_n \equiv 2\pi n/m$, at which quantum effects become important [17].

Under these assumptions, the selection of the diagrams yielding the leading contributions to the self-energy for the 2D dilute Bose gas in the normal state proceeds along similar lines as for the 3D dilute Bose gas.

Akin to the 3D case, also in 2D every *cycle* (defined as a closed path constructed by a sequence of "bare" bosonic propagators, with a common wave vector and Matsubara frequency flow) introduces a Bose function

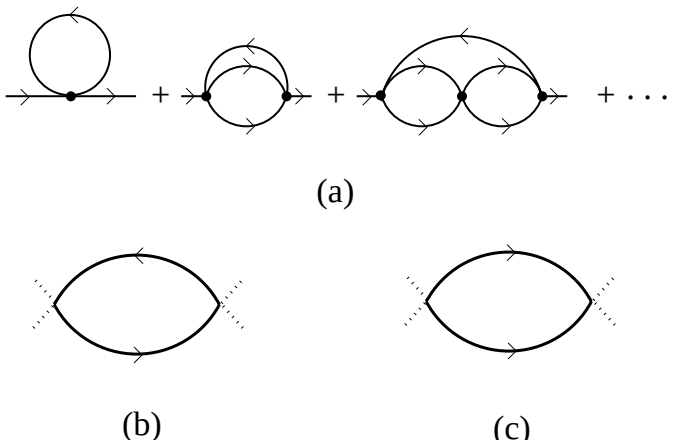

Fig. 1. (a) T-matrix approximation for the self-energy of an interacting Bose gas; (b) particle-hole bubble; (c) particle-particle bubble.

$(\mathrm{e}^{(\mathbf{q}^2/(2m)-\mu)/T}-1)^{-1}$, which appears after the summation over the common frequency running along the cycle is performed. This function, in turn, cuts off the integral over the remaining wave-vector variable approximately at $|\mathbf{q}| \simeq (mT)^{1/2}$, which is much smaller than the cutoff $1/r_0$ introduced by the potential (owing to the the diluteness condition and the assumption $T \sim T_n$).

Accordingly, the description of the dilute Bose gas retains only those diagrams with *a minimal number of cycles*, that is, just one cycle. These diagrams are shown in Figure 1a and constitute the so-called *t-matrix approximation* for the self-energy [7,18].

At $T \sim T_n$ higher-order diagrams can be estimated by replacing the bare potential by the t-matrix itself and assigning to each additional cycle a factor $t_0 \Pi_{\mathrm{ph}}(0)$. Here, t_0 and $\Pi_{\mathrm{ph}}(0)$ are the zero frequency and wave-vector values of the t-matrix and of the particle-hole bubble (Fig. 1b), respectively. It will further be shown below that the product $t_0 \Pi_{\mathrm{ph}}(0) \propto 1/\ln[1/(nr_0^2)] \ll 1$ in the dilute limit.

We will discover, however, that the classification of diagrams based on the cycle argument breaks down upon lowering the temperature down to a value T_{L}. More precisely, we will find that the t-matrix correctly describes the dilute Bose gas in the temperature range $T_{\mathrm{L}} \lesssim T \lesssim T_n$, in the sense that no other diagrams besides the t-matrix itself need to be included.

The self-energy corresponding to the set of diagrams depicted in Figure 1a reads:

$$\Sigma_t(q) = -T \sum_{\omega_{\nu'}} \int \frac{\mathrm{d}^2\mathbf{q}'}{(2\pi)^2} G(q') \left[t\left(\frac{\mathbf{q}'-\mathbf{q}}{2}, \frac{\mathbf{q}'-\mathbf{q}}{2}, q+q' \right) + t\left(\frac{\mathbf{q}-\mathbf{q}'}{2}, \frac{\mathbf{q}'-\mathbf{q}}{2}, q+q' \right) \right] \quad (2)$$

where the t-matrix $t(\mathbf{p},\mathbf{p}',P)$ is defined by the integral equation

$$t(\mathbf{p},\mathbf{p}',P) = v(\mathbf{p}-\mathbf{p}') - T \sum_{\omega_\nu} \int \frac{\mathrm{d}^2\mathbf{q}}{(2\pi)^2}\, v(\mathbf{p}-\mathbf{q}) \times G\left(\frac{P}{2}-q\right) G\left(\frac{P}{2}+q\right) t(\mathbf{q},\mathbf{p}',P) \quad (3)$$

with the notation $q \equiv (\mathbf{q}, \mathrm{i}\omega_\nu)$ ($\omega_\nu = 2\pi\nu T$ - ν integer - being a bosonic Matsubara frequency) [19].

To lowest order in the density, all single-particle Green's functions G in equations (2) and (3) are considered to be bare ones. Quite generally, self-energy insertions in the Green's functions become relevant when a phase transition is approached. It is shown in the Appendix that, in the dilute limit, the dependence of the self-energy $\Sigma_t(q)$ on q can be disregarded when calculating physical quantities, so that one may set $\Sigma_t(q) \simeq \Sigma_t(0)$ in all single-particle Green's functions entering equations (2) and (3) and re-absorb the constant $\Sigma_t(0)$ by a shift of the chemical potential. In this way, when the chemical potential is expressed in terms of n and T, one obtains

$$\mu - \Sigma_t(0) = \mu_0 \quad (4)$$

where $\mu_0 = \mu_0(n,T)$ is the chemical potential of the 2D *ideal* Bose gas [21].

In the following, we shall consider all Green's functions in equations (2) and (3) to be self-consistently dressed by the self-energy (2) with $q = 0$, resulting in an "improved" t-matrix approximation which can be adopted to approach the critical region more closely.

An explicit expression of $\Sigma_t(q)$ for arbitrary values of q is given by equation (A.7) of the Appendix, which is asymptotically valid in the dilute limit. From that expression, the shift of the chemical potential due to interaction as well as the relevant effective mass can be obtained. For the chemical potential, it is sufficient to know the value of $\Sigma_t(0)$, which from equation (A.7) becomes [20]:

$$\Sigma_t(0) \approx \frac{8\pi n}{m \ln\left[1/(m|\mu_0|r_0^2)\right]} \cdot \quad (5)$$

By entering in this expression the analytic form of the chemical potential μ_0 [21], we obtain eventually

$$\begin{aligned} \Sigma_t(0) &\approx \frac{8\pi n/m}{\ln(1/[mTr_0^2|\ln(1-\mathrm{e}^{-T_n/T})|])} \\ &\approx \frac{8\pi n/m}{\ln[1/(nr_0^2)] + \ln[T_n/(2\pi T)] - \ln|\ln(1-\mathrm{e}^{-T_n/T})|} \\ &\approx \frac{8\pi n}{m \ln\left[1/(nr_0^2)\right]} \end{aligned} \quad (6)$$

the last result holding for $T_n/\ln[1/(nr_0^2)] \ll T \lesssim T_n$, which includes the temperature range $T_{\mathrm{L}} \lesssim T \lesssim T_n$ of physical interest (the explicit expression of T_{L} being obtained in the next Sect.). Equation (6) provides the leading self-energy term for the 2D dilute Bose gas in the normal

phase, from which the shift of the chemical potential is obtained as $\mu = \mu_0 + \Sigma_t(0)$.

Note that the expression (6) is temperature independent in the temperature range $T_{\rm L} \lesssim T \lesssim T_n$ we are considering. The only temperature dependence of μ thus originates from μ_0. In particular, if we substitute the value of $T_{\rm c}$ from equation (1) into the expression (6), we obtain:

$$\begin{aligned}\mu(T_{\rm c}) &= \mu_0(T_{\rm c}) + \Sigma_t(0) \\ &\approx -\frac{2\pi n}{m\ln\left[1/(nr_0^2)\right]}\frac{1}{\ln\ln[1/(nr_0^2)]} + \frac{8\pi n}{m\ln\left[1/(nr_0^2)\right]} \\ &\approx \frac{8\pi n}{m\ln\left[1/(nr_0^2)\right]}\,, \end{aligned} \tag{7}$$

provided $\ln\ln(1/(nr_0^2)$ is sufficiently larger than unity (dilute limit). This result coincides with the value of the chemical potential obtained in references [7] and [8], where the critical temperature was approached from below.

The effective mass can eventually be calculated after analytic continuation of $\Sigma_t(q)$ given by equation (A.7). The result is:

$$\frac{m^*}{m} = 1 + \frac{1}{4\ln\ln[1/(nr_0^2)]}\,, \tag{8}$$

which holds for $T_{\rm L} \lesssim T \lesssim T_n$. Details of the derivation of equation (8) are reported in the Appendix.

3 Breakdown of the t-matrix approximation

We pass now to show that the selection of diagrams made in the previous section, which was based on the cycle argument, breaks down upon lowering the temperature. Specifically, consideration of the temperature at which the particle-hole diagrams (which where discarded by the cycle argument) are no longer negligible in comparison with the particle-particle diagrams, will lead us to identify a *lower* temperature $T_{\rm L}$, whose expression turns out to coincide with the critical temperature (1) determined in references [7] and [8] (apart from sublogarithmic corrections).

To determine the range of validity of the t-matrix approximation, it is enough to compare the particle-particle bubble $\Pi_{\rm pp}$ of Figure 1c (which constitutes the building block of the t-matrix of Figure 1a) with the *particle-hole bubble* $\Pi_{\rm ph}$ of Figure 1b. This statement follows from the classification of diagrams we have made because $t_0 \simeq \Pi_{\rm pp}(0)^{-1}$ in the dilute limit (*cf.* Eqs. (A.2) and (A.4)), yielding $\Pi_{\rm ph}(0)/\Pi_{\rm pp}(0)$ as the small parameter of the theory at $T \sim T_n$. The ratio $\Pi_{\rm ph}(0)/\Pi_{\rm pp}(0)$ grows, however, upon lowering the temperature below T_n and reaches the value of unity at the temperature $T_{\rm L}$ introduced above.

The *particle-particle bubble* is given by

$$\Pi_{\rm pp}(0) = T\sum_{\omega_\nu}\int^{r_0^{-1}} \frac{{\rm d}^2\mathbf{q}}{(2\pi)^2}\; G(q)\; G(-q) \tag{9}$$

where $G(q) = ({\rm i}\omega_\nu - \mathbf{q}^2/(2m) + \mu_0)^{-1}$ according to the arguments above. With the notation $\xi(\mathbf{q}) = |\mathbf{q}|^2/(2m) - \mu_0$, we obtain:

$$\begin{aligned}\Pi_{\rm pp}(0) &= \int^{r_0^{-1}} \frac{{\rm d}^2\mathbf{q}}{(2\pi)^2}\;\frac{1+2n_{\rm B}(\xi(\mathbf{q}))}{2\xi(\mathbf{q})} \\ &\approx \frac{m}{4\pi}\ln\left(\frac{1}{2m|\mu_0|r_0^2}\right) + \frac{1}{2\pi}\int_0^{r_0^{-1}} {\rm d}|\mathbf{q}|\;\frac{|\mathbf{q}|\,n_{\rm B}(\xi(\mathbf{q}))}{\xi(\mathbf{q})} \\ &\approx \frac{m}{4\pi}\ln\left(\frac{1}{2m|\mu_0|r_0^2}\right) \end{aligned} \tag{10}$$

where $n_{\rm B}(x) = ({\rm e}^{x/T}-1)^{-1}$ is the Bose function and the last asymptotic equality holds in the dilute limit $nr_0^2 \ll 1$ and for temperatures of the order of T_n (such that $|\mu_0| \sim T_n$).

The *particle-hole bubble* for $q = 0$ is, as usual, given by $\Pi_{\rm ph}(0) = \partial n/\partial\mu$. For the two dimensional Bose gas the chemical potential is known analytically for all temperatures and densities [21], yielding

$$\frac{\partial n}{\partial\mu} = \frac{m}{2\pi}\frac{{\rm e}^{\mu_0/T}}{1-{\rm e}^{\mu_0/T}}\,. \tag{11}$$

At $T \sim T_n$, $\mu_0(n,T_n) \sim T_n$ and $\partial n/\partial\mu \sim m$, such that the ratio $\Pi_{\rm ph}(0)/\Pi_{\rm pp}(0) \approx 1/\ln[1/(nr_0^2)] \ll 1$ in the dilute limit. When $T \ll T_n$, on the other hand, $|\mu_0| \ll T$ and $\partial n/\partial\mu \approx mT/(2\pi|\mu_0|)$, which is much larger than the corresponding value at $T \sim T_n$. A lower temperature $T_{\rm L}$ can thus be reached, such that the ratio $\Pi_{\rm ph}(0)/\Pi_{\rm pp}(0)$ equals unity when

$$\frac{1}{2}\ln\frac{1}{2m|\mu_0|r_0^2} = \frac{T_L}{|\mu_0|}\,. \tag{12}$$

Entering the asymptotic expression $|\mu_0| \approx T{\rm e}^{-T_n/T}$, which holds for $T \ll T_n$, yields eventually

$$T_{\rm L} \approx \frac{T_n}{\ln\ln[1/(nr_0^2)]} \tag{13}$$

that is valid under the assumption $\ln\ln[1/(nr_0^2)] \gg 1$ (which *defines* the diluteness condition in 2D). Our expression (13) for $T_{\rm L}$ coincides with the estimate (1) for the critical temperature given by Popov [7] and by Fisher and Hohenberg [8].

Note that the *double-log dependence* of $T_{\rm L}$ on nr_0^2 originates, on the one hand, from the log dependence of $\Pi_{\rm pp}(0)$ on $|\mu_0|$ and, on the other hand, from the exponential dependence of μ_0 on T at low temperatures. Note also that the more stringent diluteness condition $\ln\ln[1/(nr_0^2) \gg 1]$ (in the place of the original $nr_0^2 \ll 1$) is required to get a *finite* temperature range ($T_{\rm L} \lesssim T \lesssim T_n$), where self-energy diagrams can be selected by the diluteness condition.

As pointed out in the Introduction, the breakdown of the diagrammatic classification in terms of a small parameter (as explicitly seen above) finds a natural explanation as being due to the proximity to a phase transition [22]. For the 2D interacting Bose gas one knows that a Kosterlitz-Thouless superfluid transition occurs at finite

temperature [6]: the breakdown temperature $T_{\rm L}$ is thus expected to provide an upper estimate for the superfluid critical temperature $T_{\rm c}$.

The fact that the upper boundary $T_{\rm L}$ turns out to be very close to $T_{\rm c}$ is further confirmed by applying the same sort of arguments to the 3D dilute Bose gas, for which Monte Carlo results are available [15,16]. In this case, the particle-particle and particle-hole bubbles are given, respectively, by

$$\Pi_{\rm pp}(0) \approx \frac{m}{2\pi^2 r_0} = \frac{m}{4\pi a} \tag{14}$$

where a is the scattering length, and

$$\Pi_{\rm ph}(0) = \frac{\partial n}{\partial \mu} \approx \frac{2mn^{1/3}}{3\zeta(3/2)^{4/3}} \frac{T_{\rm BE}}{T - T_{\rm BE}} \tag{15}$$

since $\mu_0 \simeq -9\zeta(3/2)^2 (T - T_{\rm BE})^2/(16\pi T_{\rm BE})$ for the chemical potential of the ideal Bose gas (valid near the Bose-Einstein temperature $T_{\rm BE} = 2\pi/\zeta(3/2)^{2/3} n^{2/3}/m$). The temperature at which these contributions coincide then defines the 3D breakdown temperature $T_{\rm L}^{3D}$. One obtains:

$$\frac{T_{\rm L}^{3D} - T_{\rm BE}}{T_{\rm BE}} = \frac{8\pi}{3\zeta(3/2)^{4/3}} n^{1/3} a \simeq 2.33\, n^{1/3} a\,. \tag{16}$$

This result for the breakdown temperature $T_{\rm L}$ is remarkably close to the value for the critical temperature of the 3D hard-core Bose gas in the dilute limit obtained by Monte Carlo simulations [16], which yields $(T_{\rm c} - T_{\rm BE})/T_{\rm BE} = (2.3 \pm 0.25) n^{1/3} a$, and coincides with the analytic result of reference [23], which was obtained by a completely different method. Very recent Monte Carlo simulations [24,25] have found instead a smaller value 1.3 for the coefficient of the linear dependence of the shift of the critical temperature on the gas parameter $n^{1/3}a$. It has been pointed out, however, in reference [26] that, while in reference [16] the coefficient of the linear dependence has been calculated after carefully taking the limit $n^{1/3}a \to 0$, in references [24] and [25] the coefficient has been obtained by direct extrapolation of the results obtained at finite density. According to reference [26], this procedure is affected by subleading logarithmic contributions, which are negligible only at densities much smaller than those explored in references [24] and [25]. In any case, we remark that both the results of references [24] and [25], as well as of reference [16], are consistent with our claim that $T_{\rm L}$ constitutes an upper boundary for the actual $T_{\rm c}$.

The result (16) should be regarded as altogether non trivial, since previous analytic treatments of the 3D dilute Bose gas resulted either in different dependences of $(T_{\rm c} - T_{\rm BE})/T_{\rm BE}$ on the parameter $n^{1/3}a$, *e.g.*, of the type $(n^{1/3}a)^{1/2}$ [*cf.* Ref. [27]] or $(n^{1/3}a)^{2/3}$ [*cf.* Ref. [28]], or in the same linear dependence on the parameter $n^{1/3}a$, but with a different proportionality coefficient [29–31]. In our approach, the linear dependence on the parameter $n^{1/3}a$ of the temperature shift has been directly related to the quadratic dependence of the free-boson chemical potential on $T - T_{\rm BE}$ near $T_{\rm BE}$ in 3D.

4 Concluding remarks

In this paper, we have considered the two-dimensional dilute Bose gas in the normal phase, in the interesting temperature region ranging from an *upper* temperature T_n (below which quantum effects become important) to a *lower* temperature $T_{\rm L}$ (which we have identified as an upper limit to the critical temperature). In this temperature region we have analyzed the ordinary diagrammatic theory and organized it in powers of the parameter $1/\ln[1/(nr_0^2)]$, which was assumed to be small compared to unity.

In this way, the standard t-matrix has been identified as yielding the dominant set of diagrams for the self-energy when $nr_0^2 \ll 1$. Further analysis of the theory to define the temperature range where the t-matrix approximation holds has, however, led us to consider the stronger condition $\ln\ln[1/(na^2)] \gg 1$ as characteristic of the "dilute" Bose gas in two dimensions, thus confirming the criterion introduced by Fisher and Hohenberg [8] *via* different methods.

Our identification of the lower temperature $T_{\rm L}$ rests on the finding that the diagrammatic classification scheme for the 2D dilute Bose gas breaks down at this lower temperature, in the sense that additional diagrams (besides the t-matrix) become also important at $T_{\rm L}$ and the hierarchy established for the dilute gas no longer holds. In this respect, it may be worth mentioning that by our scheme the critical temperature cannot be obtained *via* the usual criterion which defines $T_{\rm c}(n)$ as the temperature where the equation $\mu(n, T_{\rm c}) = \Sigma(q = 0; n, T_{\rm c})$ is satisfied. Solving, in fact, for this equation would require one to rely on an approximation for the self-energy which is valid *even at* $T_{\rm c}$. We have seen, however, that in our case the t-matrix approximation for the self-energy breaks down *before* reaching $T_{\rm c}$, as soon as the critical region above $T_{\rm c}$ is approached.

The finding that an upper boundary to the superfluid critical temperature can be obtained from ordinary diagrammatic methods in the normal phase, both in two and three dimensions, constitutes *per se* a nontrivial result, especially because the nature of the (superfluid) transition in two and three dimensions is quite different (involving, respectively, quasi-long-range order and true long-range order).

In addition, our approach is rather straightforward and amenable to direct implementation to more complex physical situations. In this respect, a possible application of our results may be the normal state of high-temperature cuprate superconductors, which are quasi-two-dimensional systems. Experiments related to the normal [32,33] and superconducting [34] state in these systems suggest, in fact, that a correct description of their properties might require an intermediate (crossover) approach between the Fermi liquid theory (weak-coupling) and the dilute Bose gas approach (strong-coupling). For this reason, crossover theories have been considered by several authors, both for the normal state [35,36] and the broken-symmetry phase [37,38]. Since a reliable study of the crossover problem should require a good knowledge of

at least the extreme (weak- and strong-coupling) limits, the approach developed in this paper might shed light on the strong-coupling limit of these theories [9].

We are indebted to C. Castellani, P. Nozières, and F. Pistolesi for helpful discussions. I.T. gratefully acknowledges financial support from the Italian INFM under contract No. PRA-HTSC/96-99.

Appendix A

In this Appendix, we obtain an analytic expression for the t-matrix self-energy, which is valid above $T_{\rm L}$ in the dilute limit. From this expression, the effective mass (at $\mathbf{q}=0$) is calculated. In addition, the approximation

$$\Sigma_t(q) \simeq \Sigma_t(0) \tag{A.1}$$

(which is crucial for the arguments presented in the text) will be justified theoretically and checked numerically. Both two-dimensional and three-dimensional cases will be considered for completeness.

A1. Two dimensions

It is convenient to parametrize the short-range potential appearing in the t-matrix integral equation (3) by a separable potential in wave-vector space, by letting $v(\mathbf{p}-\mathbf{p}') \to v_0 w_{\mathbf{p}} w_{\mathbf{p}'}$ with $w_{\mathbf{p}} = \theta(k_0 - |\mathbf{p}|)$ and $k_0 = r_0^{-1}$. The use of a separable potential in the t-matrix integral equation (3) is justified for $|\mathbf{p}|, |\mathbf{p}'| \ll k_0$, because in this range both the original potential and the separable potential are constant and equal to v_0. For a dilute Bose gas, at $T \sim T_n$, the relevant wave vectors, in fact, are smaller or at most of the order of $n^{1/D} \ll k_0 = 1/r_0$, thus justifying the use of a separable potential within this wave-vector range. Equation (3) can therefore be readily solved to yield $t(\mathbf{p},\mathbf{p}',P) = w_{\mathbf{p}} w_{\mathbf{p}'} t(P)$, with

$$t^{-1}(P) = v_0^{-1} + T\sum_{\omega_\nu} \int \frac{{\rm d}^2\mathbf{q}}{(2\pi)^2}\, w_{\mathbf{q}}^2 G\left(\frac{P}{2}-q\right) G\left(\frac{P}{2}+q\right), \tag{A.2}$$

where $G(q) = ({\rm i}\omega_\nu - \mathbf{q}^2/2m + \mu_0)^{-1}$, consistently with the assumption (A.1) and the ensuing equation (4). This choice of $G(q)$ will lead us to verify the key assumption (A.1) in a self-consistent manner. The frequency sum in equation (A.2) can be performed explicitly, yielding

$$T\sum_{\omega_\nu} \int \frac{{\rm d}^2\mathbf{q}}{(2\pi)^2}\, w_{\mathbf{q}}^2\, G\left(\frac{P}{2}-q\right) G\left(\frac{P}{2}+q\right) = \int \frac{{\rm d}^2\mathbf{q}}{(2\pi)^2} w_{\mathbf{q}}^2 \, \frac{1+n_{\rm B}(\xi_{\mathbf{P}/2-\mathbf{q}})+n_{\rm B}(\xi_{\mathbf{P}/2+\mathbf{q}})}{\mathbf{P}^2/(4m)+\mathbf{q}^2/m - 2\mu_0 - {\rm i}\Omega_\nu}\,. \tag{A.3}$$

In the dilute limit ($nr_0^2 \ll 1$) and for $T_{\rm L} \lesssim T \lesssim T_n$, the Bose functions appearing in the above expression can be neglected, since they yield contributions smaller by a factor $Tr_0^2 \ll 1$ with respect to the term retained. The integration over the wave vector $\mathbf{q}$ then yields

$$t^{-1}(P) = \frac{1}{v_0} + \frac{m}{4\pi} \ln\left[\frac{k_0^2/m + 2|\mu_0| + \mathbf{P}^2/(4m) - {\rm i}\Omega_\nu}{2|\mu_0| + \mathbf{P}^2/(4m) - {\rm i}\Omega_\nu}\right] \tag{A.4}$$

where ln stands for the principal branch of the complex logarithm. The t-matrix self-energy is obtained by inserting expression (A.4) into equation (2) which, for a separable potential, becomes

$$\Sigma_t(\mathbf{q},\omega_\nu) = -2\,T\sum_{\Omega_{\nu'}} \int \frac{{\rm d}^2\mathbf{q}'}{(2\pi)^2}\, w^2_{(\mathbf{q}'-\mathbf{q})/2} \times G(\mathbf{q}', \Omega_{\nu'} - \omega_\nu) t(\mathbf{q}+\mathbf{q}', \Omega_{\nu'}). \tag{A.5}$$

To perform the frequency sum in equation (A.5) we exploit the analytic properties of $t(\mathbf{P},z)$. From equation (A.4), after the replacement ${\rm i}\Omega_{\nu'} \to z$, it can be readily verified that $t(\mathbf{P},z)$ has a simple pole for $z = \mathbf{P}^2/(4m) + 2|\mu_0| + k_0^2/[m(1-{\rm e}^{-1/\tilde{v}_0})]$ (with $\tilde{v}_0 = mv_0/(4\pi)$) and a branch cut along the real axis for $\mathbf{P}^2/(4m) + 2|\mu_0| < {\rm Re}(z) < \mathbf{P}^2/(4m) + 2|\mu_0| + k_0^2/m$. The frequency sum in equation (A.5) can be then performed by a contour integration, yielding three distinct contributions: one from the simple pole of the Green's function $G(\mathbf{q}',z)$, one from the simple pole of the t-matrix, and one from the integration along the cut of $t(\mathbf{q}+\mathbf{q}',z)$. The term originating from the simple pole of the t-matrix, which occurs for ${\rm Re}(z) > k_0^2/m$, is exponentially suppressed by the Bose factor $1/(\exp(\beta z)-1)$ and is thus negligible. The term associated with the integration along the cut can be estimated to be smaller than the term from the simple pole of the Green's function by a factor $1/\ln[1/(nr_0^2)]$, and is also negligible in the dilute limit. We are thus left with the expression:

$$\Sigma_t(\mathbf{q},\omega_\nu) = 2\int \frac{{\rm d}^2\mathbf{p}}{(2\pi)^2} \frac{w^2_{\mathbf{q}/2}}{{\rm e}^{\beta[\frac{(\mathbf{q}-\mathbf{p})^2}{2m}+|\mu_0|]}-1} \left[\frac{1}{v_0} + \frac{m}{4\pi} \times \ln\frac{k_0^2/m + |\mu_0| + \mathbf{q}^2/(2m) - \mathbf{p}^2/(4m) - {\rm i}\omega_\nu}{|\mu_0| + \mathbf{q}^2/(2m) - \mathbf{p}^2/(4m) - {\rm i}\omega_\nu}\right]^{-1}. \tag{A.6}$$

Note that the Bose factor in equation (A.6) is peaked about $\mathbf{p}=\mathbf{q}$ with a width of order $T^{1/2}$, which is smaller than the range of $\mathbf{p}$ over which the log-term in the denominator of equation (A.6) varies appreciably. When performing the integration over $\mathbf{p}$ in equation (A.6), we can then approximate $\mathbf{p}=\mathbf{q}$ in the logarithm, which is in this way factored out of the integral, yielding the following asymptotic expression for the self-energy:

$$\frac{\Sigma_t(q)}{2n} \approx w^2_{\mathbf{q}/2}\left\{\frac{1}{v_0} + \frac{m}{4\pi}\ln\left[\frac{k_0^2/m + |\mu_0| + \mathbf{q}^2/(4m) - {\rm i}\omega_\nu}{|\mu_0| + \mathbf{q}^2/(4m) - {\rm i}\omega_\nu}\right]\right\}^{-1}. \tag{A.7}$$

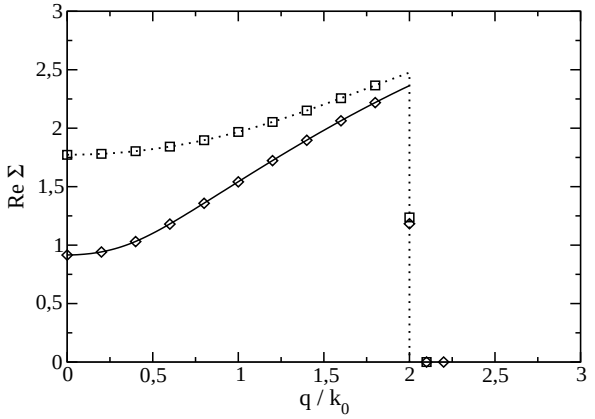

(a)

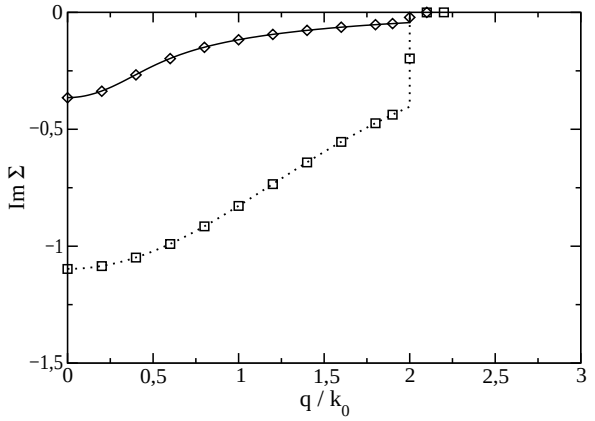

(b)

Fig. 2. $\Sigma(q,\omega_\nu)$ (units of T_n) for a 2D dilute Bose gas at $T = T_n$ and $nr_0^2 = 1.6 \times 10^{-3}$. Numerical results for $\nu = 10$ (diamonds) and $\nu = 100$ (squares) are compared with the analytic expression (A.7) (full and dotted lines, respectively).

The analytic expression (A.7) can be compared with the numerical calculation for the t-matrix self-energy, obtained by retaining all contributions to equation (A.5).

We have found that the asymptotic expression (A.7) reproduces extremely well the numerical results for (A.5) when the diluteness parameter is sufficiently small. As an example, in Figure 2 the analytic expression for $\Sigma_t(q)$ is compared with the numerical results for the choice of parameters $T = T_n$, $mv_0/(4\pi) = 1$, and $nr_0^2 = 1.6 \times 10^{-3}$. One can see that in this case the agreement is excellent.

The expression (A.7) for the self-energy can also be used to verify that, when evaluating physical quantities (such as the density n), the wave-vector and frequency dependence of $\Sigma_t(q)$ is actually irrelevant, so that one can approximate $\Sigma_t(q) \simeq \Sigma_t(0)$ as anticipated in equation (A.1). This is because the presence of the logarithm in equation (A.7) makes the dependence of $\Sigma_t(q)$ on q rather slow. The approximation $\Sigma_t(q) \simeq \Sigma_t(0)$ is thus justified over a large portion of q space and can be exploited to evaluate physical quantities. In particular, for $T = T_n$ we have obtained numerically that the relative error when evaluating $n = -T\sum_\nu \int \frac{\mathrm{d}^2\mathbf{q}}{(2\pi)^2}\, G(q)$ alternatively with $G(q) = [\mathrm{i}\Omega_\nu - \mathbf{q}^2/(2m) + \mu - \Sigma_t(q)]^{-1}$ or with $G(q) \to G_0(q) = [\mathrm{i}\Omega_\nu - \mathbf{q}^2/(2m) + \mu - \Sigma_t(0)]^{-1}$ is less than 1% for $nr_0^2 \lesssim 10^{-2}$.

Finally, the t-matrix self-energy (A.7) can be exploited to calculate the effective mass for the dilute Bose gas. Recall that, once the retarded self-energy is known, the effective mass can be calculated as [39]

$$\frac{m^*}{m} = \left(1 - \frac{\partial \mathrm{Re}\Sigma(|\mathbf{q}|,\omega)}{\partial\omega}\right)\left[1 + \frac{m}{|\mathbf{q}|}\frac{\partial \mathrm{Re}\Sigma(|\mathbf{q}|,\omega)}{\partial|\mathbf{q}|}\right]^{-1}, \tag{A.8}$$

where the derivatives are meant to be calculated at the quasi-particle pole defined by the equation

$$\omega_{\mathbf{q}} = \frac{\mathbf{q}^2}{2m} - \mu + \mathrm{Re}\Sigma(\mathbf{q},\omega_{\mathbf{q}}). \tag{A.9}$$

In general, the effective mass m^* depends on $\mathbf{q}$. Here we are interested in its value at $\mathbf{q} = 0$, which is relevant at low temperatures.

The self-energy (A.7) can be analytically continued *via* the replacement $\mathrm{i}\omega_n \to \omega + \mathrm{i}0^+$. The quasi-particle-pole equation (A.9) at $\mathbf{q} = 0$ can then be solved asymptotically, to yield

$$\omega_0 = -\mu + \Sigma_t(0)\left(1 - 2\frac{\ln\ln[1/(nr_0^2)]}{\ln(1/(nr_0^2)]}\right) \tag{A.10}$$

as it can be verified by inserting the value (A.10) for ω_0 in the quasi-particle-pole equation and by discarding subleading terms in the dilute limit $nr_0^2 \ll 1$. The derivatives of $\Sigma(\mathbf{q},\omega)$ at $(\mathbf{q} = 0, \omega = \omega_0)$ can also be readily calculated. The effective mass at $\mathbf{q} = 0$ is then given by

$$\begin{aligned}\frac{m^*}{m} &\approx \frac{1 + 1/(2\ln\ln[1/(nr_0^2)])}{1 - 1/(4\ln\ln[1/(nr_0^2)])} \\ &\approx 1 + 1/(4\ln\ln[1/(nr_0^2)]).\end{aligned} \tag{A.11}$$

Note the occurrence of the same double-log dependence characteristic of the temperature T_L.

A2. Three dimensions

The three-dimensional case can be treated in a parallel fashion to the two-dimensional case. By considering the same separable potential adopted in 2D, and by following the same steps which lead to equation (A.4), we now obtain:

$$\begin{aligned}t^{-1}(P) = \frac{1}{v_0} + \frac{m}{2\pi^2}\Bigg[k_0 - m^{1/2}\sqrt{-2\mu_0 + \frac{\mathbf{P}^2}{4m} - \mathrm{i}\Omega_\nu} \\ \times \arctan\frac{k_0/m^{1/2}}{\sqrt{-2\mu_0 + \frac{\mathbf{P}^2}{4m} - \mathrm{i}\Omega_\nu}}\Bigg]\end{aligned} \tag{A.12}$$

where the complex arctan is defined, as usual, in terms of the principal branch of the complex logarithm as follows:

$$\arctan z = \frac{\mathrm{i}}{2} \ln \frac{1 - \mathrm{i}z}{1 + \mathrm{i}z} \cdot \tag{A.13}$$

Like in 2D, the t-matrix $t(\mathbf{P}, z)$ has a branch cut along the real axis for $\mathbf{P}^2/(4m) + 2|\mu_0| < \mathrm{Re}(z) < \mathbf{P}^2/(4m) + 2|\mu_0| + k_0^2/m$, and a simple pole located along the real axis for $\mathrm{Re}z > \mathbf{P}^2/(4m) + 2|\mu_0| + k_0^2/m$. Upon transforming the frequency sum in (A.5) into a contour integration, the t-matrix simple pole contribution will be again strongly suppressed by the Bose factor, while the term associated with the integration along the cut can now be proven to be smaller than the term originating from the simple pole of the Green's function by a factor $(nr_0^3)^{1/2}$. In the dilute limit, only the simple pole of the Green's function therefore contributes to the contour integration. By the same argument leading to equation (A.7), we obtain the following asymptotic expression for the t-matrix self-energy:

$$\frac{\Sigma_t(q)}{2n} \approx w_{\mathbf{q}/2}^2 \left[\frac{1}{v_0} + \frac{m}{2\pi^2} \left(k_0 - \sqrt{|\mu_0| + \frac{\mathbf{q}^2}{4m} - \mathrm{i}\omega_\nu} \right. \right. \\ \left. \left. \times\, m^{1/2} \arctan \frac{k_0/m^{1/2}}{\sqrt{|\mu_0| + \frac{\mathbf{q}^2}{4m} - \mathrm{i}\omega_\nu}} \right) \right]^{-1} \cdot \tag{A.14}$$

The asymptotic expression (A.14) has also been checked against numerical calculation of equation (A.5) in three dimensions. In Figure 3 the analytic expression (A.14) is compared with the numerical results for the choice of parameters $T = T_n$, $(2\pi^2)/(mv_0k_0) \to 0$, and $n^{1/3}r_0 = 1 \times 10^{-2}$. Even in 3D the agreement is excellent.

The approximation $\Sigma_t(q) \simeq \Sigma(0)$ has further been checked by evaluating the particle density. In this case, we have found that the error introduced by the approximation (A.1) in the estimate for the density is less than 1% when $nr_0^3 \lesssim 5 \times 10^{-3}$.

Finally, the solution of the quasi-particle-pole equation (A.9) at $\mathbf{q} = 0$ in 3D is given by

$$\omega_0 = -\mu + \Sigma_t(0) = |\mu_0|, \tag{A.15}$$

while the retarded self-energy near the quasi-particle pole is given by

$$\Sigma(\mathbf{q}, \omega) = \frac{2n}{\frac{m}{4\pi a} - \mathrm{i}\frac{m}{2\pi^2} A(\mathbf{q}, \omega) \left[\frac{\pi}{2} + \frac{\mathrm{i}}{2} \ln \frac{\pi/(2aA(\mathbf{q},\omega)) + 1}{\pi/(2aA(\mathbf{q},\omega)) - 1} \right]} \tag{A.16}$$

with $A(\mathbf{q}, \omega) = \sqrt{\omega - \mathbf{q}^2/(4m) - |\mu_0|}$ and where we have introduced the scattering length a *via* the relation $m/(4\pi a) \approx (mk_0)/(2\pi^2)$. By using the definition (A.8), the effective mass at $\mathbf{q} = 0$ can be readily calculated, leading to the result:

$$\frac{m^*}{m} \approx \left[1 + \frac{8\pi n a^3}{m} \left(1 + \frac{4}{\pi^2} \right) \right] \left[1 + \frac{4\pi n a^3}{m} \left(1 + \frac{4}{\pi^2} \right) \right]^{-1} \\ \approx 1 + \frac{4\pi n a^3}{m} \left(1 + \frac{4}{\pi^2} \right) \cdot \tag{A.17}$$

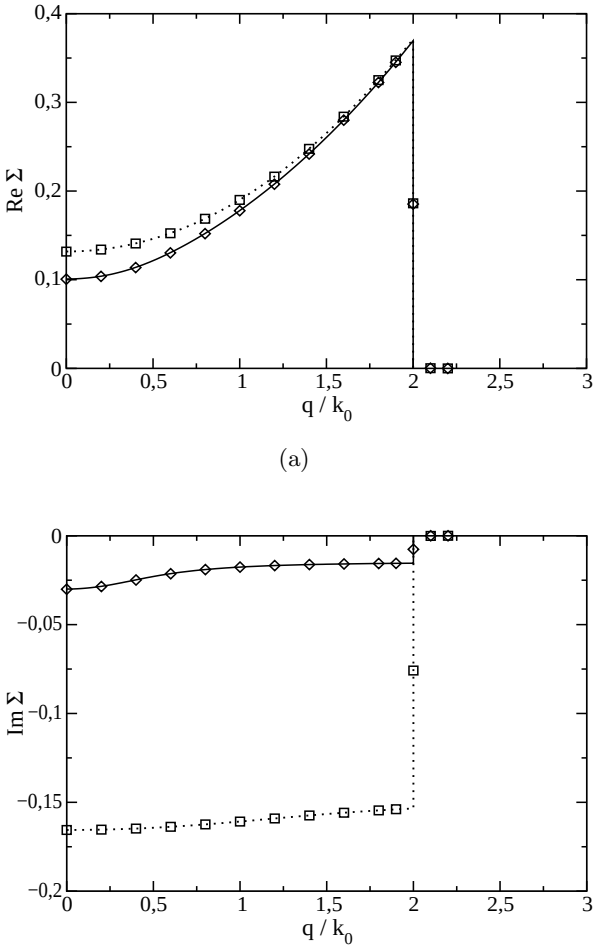

Fig. 3. $\Sigma(q, \omega_\nu)$ (units of T_n) for a 3D dilute Bose gas at $T = T_n$ and $n^{1/3}r_0 = 1 \times 10^{-2}$. Numerical results for $\nu = 10$ (diamonds) and $\nu = 100$ (squares) are compared with the analytic expression (A.14) (full and dotted lines, respectively).

Note that the interaction increases the (quasi)-particle mass both in 3D and in 2D with respect to its bare value.

References

1. W.D. McCornick, D.L. Goodstein, J.G. Dash, Phys. Rev. **168**, 249 (1968); G.A. Stewart, J.G. Dash, Phys. Rev. A **2**, 918 (1970); J.G. Dash, Phys. Rep. C **38**, 177 (1978); D.J. Bishop, J.D. Reppy, Phys. Rev. B **22**, 5171 (1980).
2. L.J. Lantto, R.M. Nieminen, J. Low Temp. Phys. **37**, 1 (1979).
3. M.H. Anderson *et al.*, Science **269**, 198 (1995); C.C. Bradley *et al.*, Phys. Rev. Lett. **75**, 1687 (1995); K.B. Davis *et al.*, Phys. Rev. Lett. **75**, 3969 (1995).
4. D.G. Fried *et al.*, Phys. Rev. Lett. **81**, 3811 (1998).

5. For a review, see F. Dalfovo, S. Giorgini, L.P. Pitaevskii, S. Stringari, Rev. Mod. Phys. **71**, 463 (1999).
6. J.M. Kosterlitz, D.J. Thouless, J. Phys. C **6**, 1181 (1973).
7. V.N. Popov, *Functional Integrals in Quantum Field Theory and Statistical Physics* (Riedel, Dordrecht, 1983); *Functional Integrals and Collective Excitations* (Cambridge University Press, Cambridge, 1987).
8. D.S. Fisher, P.C. Hohenberg, Phys. Rev. B **37**, 4936 (1988).
9. P. Pieri, G.C. Strinati, I. Tifrea (in preparation).
10. M. Schick, Phys. Rev. A **3**, 1067 (1971).
11. D.F. Hines, N.E. Frankel, D.J. Mitchell, Phys. Lett. **68 A**, 12 (1978).
12. E.B. Kolomeisky, J.P. Straley, Phys. Rev. B **46**, 11749 (1992).
13. E.H. Lieb, J. Yngvason, J. Stat. Phys. **103**, 509 (2001), `math-ph/0002014`.
14. C. Chang, R. Friedberg, Phys. Rev. B **51**, 1117 (1995).
15. P. Grüter, D. Ceperley, F. Laloë, Phys. Rev. Lett. **79**, 3549 (1997).
16. M. Holzmann, W. Krauth, Phys. Rev. Lett. **83**, 2687 (1999).
17. R.M. May, Phys. Rev. **115**, 254 (1959).
18. S.T. Beliaev, JETP **34**, 417 (1958) [Sov. Phys. JETP **7**, 289 (1958)].
19. The interaction vertices represented by points in the diagrams of Figure 1 are meant to be symmetrized: $v(\mathbf{q}_1,\mathbf{q}_2,\mathbf{q}_3,\mathbf{q}_4) = v(\mathbf{q}_1-\mathbf{q}_3)+v(\mathbf{q}_1-\mathbf{q}_4)$. By expressing the self-energy diagrams of Figure 1a in terms of unsymmetrized interaction vertices and taking into account the symmetry factor of these diagrams, equations (2) and (3) follow.
20. Throughout this paper, we adopted the same notation of reference [8], with the symbol $\approx$ meaning "asymptotically equal".
21. In two dimensions, the chemical potential of the ideal Bose gas can be evaluated analytically for *all* temperatures and densities, yielding $\mu_0(n,T) = T\ln(1-\mathrm{e}^{-2\pi n/mT})$ (*cf.* Ref. [17]).
22. In a recent paper (W.J. Mullin, M. Holzmann, F. Laloë, J. Low Temp. Phys. **121**, 269 (2000)), the method of Ursell operators has been applied to the 2D dilute Bose gas in the normal phase. Interestingly, an instability in the solution of the integral equation for the one-particle reduced density has been found, which has been also intepreted as due to the proximity to a phase transition.
23. G. Baym, J.-P. Blaizot, J. Zinn-Justin, Europhys. Lett. **49**, 150 (2000).
24. V. Kashurnikov, N. Prokofèv, B. Svistunov, `cond-mat/0103149`.
25. P. Arnold, G. Moore, `cond-mat/0103228`.
26. M. Holzmann, G. Baym, F. Lalöe, `cond-mat/0103595`.
27. K. Huang, Phys. Rev. Lett. **83**, 3770 (1999).
28. H.T.C. Stoof, Phys. Rev. Lett. **66**, 3148 (1991).
29. T.D. Lee, C.N. Yang, Phys. Rev. **112**, 1419 (1958).
30. H.T.C. Stoof, Phys. Rev. A **45**, 8398 (1992).
31. G. Baym, J.-P. Blaizot, M. Holzmann, F. Lalöe, D. Vautherin, Phys. Rev. Lett. **83**, 1773 (1999).
32. H. Ding *et al.*, Nature **382**, 51 (1996); Phys. Rev. Lett. **78**, 2628 (1997).
33. A.G. Loeser *et al.*, Science **273**, 325 (1996).
34. Y.J. Uemura *et al.*, Phys. Rev. Lett. **62**, 2317 (1989).
35. R. Haussmann, Z. Phys. B **91**, 291 (1993).
36. P. Pieri, G.C. Strinati, Phys. Rev. B. **61**, 15370 (2000).
37. M. Randeria, Ji-Min Duan, Lih-Yir Shieh, Phys. Rev. Lett. **62**, 981 (1989); Phys. Rev. B **41**, 327 (1990).
38. F. Pistolesi, G.C. Strinati, Phys. Rev. B **53**, 15168 (1996).
39. J.W. Negele, H. Orland, *Quantum Many-Particle Systems* (Addison-Wesley, New York, 1988), Sect. 5.3.